A relativistic beam-plasma system with electromagnetic waves

E. G. Evstatiev, P. J. Morrison, and W. Horton
Department of Physics and Institute for Fusion Studies, The University of Texas at Austin, Austin, Texas 78712

(Received 2 March 2005; accepted 23 May 2005; published online 29 June 2005)

A nonlinear multiwave model that describes the interaction of an electron beam, plasma waves, and electromagnetic waves in a cold plasma is derived and studied. The derivation, which is based on slow amplitude and phase change approximations, begins with the electromagnetic Lagrangian coupled to an electron beam, a background plasma, and electrostatic and electromagnetic waves. The model obtained is finite dimensional, and allows for efficient computational and analytical study. Numerical computations demonstrate that with the inclusion of an electromagnetic wave with the plasma wave, the beam-plasma instability is suppressed. If two electromagnetic waves that satisfy a beat-wave matching condition are included, the plasma wave is seen to be amplified provided the beat-wave amplitude exceeds a certain threshold. © *2005 American Institute of Physics*. [DOI: 10.1063/1.1950127]

I. INTRODUCTION

The main purpose of this paper is to construct a simplified model for relativistic wave-particle interactions. Wave-particle interactions are of basic importance in plasma physics and are universal phenomena in space and laboratory plasmas. Of particular interest is the application to both plasma-based accelerators and laser wakefield accelerators, and the present work provides a theoretical method for modeling features of both kinds of accelerator schemes. The model describes beam excited plasma waves in both the linear and the nonlinear stages, with the inclusion of the effect of electromagnetic waves (the laser) in the system. The model generalizes the so-called single wave model[1–3] by simultaneously including relativistic effects, multiple waves, both plasma (electrostatic) and electromagnetic, and three spatial dimensions.

The derivation proceeds from the relativistic action principle for particles coupled to Maxwell's equations, and the reduction procedure developed results in model equations that inherit Lagrangian and Hamiltonian structure. Thus, the second purpose of this paper is to demonstrate how to systematically do such derivations. Action principles and their uses in plasma physics have previously been discussed in, e.g., Refs. 4–9 in a variety of contexts. In our context, the partial differential equations that describe a continuous beam-plasma system are reduced to a finite degree-of-freedom system. This new system conserves energy and the total momentum of particles and waves (both plasma and electromagnetic), which is a measure of self-consistency. The model allows for computational efficiency and, with additional simplifications, for analytical treatment.

Although the model can be used to study the interaction of beam particles, plasma waves, and external electromagnetic waves in a general context of laser-plasma interaction, the third purpose of the paper is to analyze some simplified cases. Given that the beam particles have velocity nearly equal to the plasma wave phase velocity (resonant particles), the model describes an efficient means of energy transfer between the electromagnetic (laser) waves and the plasma wave. This example suggests that this energy transfer can be used in plasma-based accelerators to further increase the energy of the accelerated particles. Even with small intensity of the laser pulse, a considerable amount of energy can be transferred; for our initial conditions the plasma wave has an increase in amplitude of about 6%. Numerical studies using the model show that before such a transfer can occur, the electromagnetic wave amplitudes must exceed a certain threshold.

The structure of the paper is as follows. Section II is dedicated to the derivation of the model, which is a significant generalization of the nonrelativistic model of Ref. 10. Here the basic approximations and ideas that underlie the derivation are described. Limitations are discussed and justification of the approximations used are given. Also, in this section the Hamiltonian form and conservation laws are described. In Sec. III, we study a simplification of the model in which one plasma and one or two electromagnetic waves are retained. With one electromagnetic wave there is no resonant interaction, but the electromagnetic wave behaves as an external force acting on the beam-plasma system that leads to suppression of the beam-plasma instability. With two electromagnetic waves energy transfer between the plasma and the electromagnetic waves occurs when a matching condition is satisfied, provided the electromagnetic waves have amplitudes that are larger than a certain threshold. In Sec. IV we conclude.

II. DERIVATION

We begin by assuming the presence of a background plasma with dynamics that responds linearly and nonrelativistically to the presence of waves. The ions of the background plasma are assumed to be immobile. These are good approximations because the resonant particles are assumed to constitute a very small fraction of the total plasma, and their velocities are assumed to be much larger than the thermal velocity of the background plasma. Both plasma waves and

electromagnetic waves are allowed, with the latter having a frequency of oscillation of the order of a few times the plasma frequency. This is the justification for the neglect of the ions. The external electric fields are assumed small enough so that nonlinear effects in the background plasma can be neglected. This will be shown to be the case when we consider particular parameter ranges.

A. Derivation of the relativistic model

The action principle for the system is a field theoretic generalization of Hamilton's principle (see, e.g., Ref. 9) $S=\int L dt$, where Lagrangian L for the system of fields, background plasma, and relativistic beam particles is given by

$$L=\int d^3x\left\{\frac{1}{2}mn|\mathbf{v}|^2+\frac{1}{8\pi}\left(\left|\nabla\phi+\frac{1}{c}\frac{\partial\mathbf{A}}{\partial t}\right|^2-|\nabla\times\mathbf{A}|^2\right)-\rho\phi+\frac{1}{c}\mathbf{j}\cdot\mathbf{A}\right\}+\sum_{j=1}^{N}\left\{-mc^2\sqrt{1-\frac{\dot{\mathbf{r}}_j^2}{c^2}}+e\phi(\mathbf{r}_j,t)-\frac{e}{c}\dot{\mathbf{r}}_j\cdot\mathbf{A}(\mathbf{r}_j,t)\right\}. \tag{1}$$

Here $\mathbf{v}$ and n are the Eulerian velocity field and particle density of the background plasma, respectively, ϕ and $\mathbf{A}$ are the scalar and vector potentials associated with the N_L electrostatic and N_T electromagnetic waves, respectively, N is the number of beam particles, $\mathbf{j}$ is the current, ρ is the charge density, and $-e$ is the electron charge. Quantities with a subscript refer to particles whereas those without refer to the background plasma. The Coulomb gauge $\nabla\cdot\mathbf{A}=0$ is assumed.

Using fluid theory, the linear response of the background plasma is given by

$$\rho=-\frac{1}{4\pi}\nabla^2\phi,\qquad \mathbf{j}_L=\frac{1}{4\pi}\nabla\frac{\partial\phi}{\partial t},\qquad \mathbf{j}_T=-\frac{c}{4\pi}\left(\nabla^2\mathbf{A}-\frac{1}{c^2}\frac{\partial^2\mathbf{A}}{\partial t^2}\right),\qquad \mathbf{v}=-\frac{1}{ne}\mathbf{j}, \tag{2}$$

where $\mathbf{j}_L$ and $\mathbf{j}_T$ are the longitudinal and transverse parts of the current. The first three equations of Eq. (2) follow directly from Maxwell equations upon splitting the current into irrotational and solenoidal parts and using the Coulomb gauge (see, e.g., Ref. 11). Substituting the above relations into the Lagrangian (1) is inexact because it amounts to the neglect of the fields due to the beam particles. We return to the justification for this and other approximations at the end of this section.

Suppose that the electrostatic and vector potentials are represented by three-dimensional Fourier series as

$$\phi(\mathbf{r},t)=\sum_{\mathbf{k}_L>0}\left(f_{\mathbf{k}_L}e^{i\mathbf{k}_L\cdot\mathbf{r}}+f_{\mathbf{k}_L}^*e^{-i\mathbf{k}_L\cdot\mathbf{r}}\right), \tag{3}$$

$$\mathbf{A}(\mathbf{r},t)=\sum_{\mathbf{k}>0}\left(\mathbf{a}_{\mathbf{k}}e^{i\mathbf{k}\cdot\mathbf{r}}+\mathbf{a}_{\mathbf{k}}^*e^{-i\mathbf{k}\cdot\mathbf{r}}\right), \tag{4}$$

where the asterisk superscript denotes the complex conjugate. The sums $\mathbf{k}_L>0$ and $\mathbf{k}>0$ range over half of the corresponding wave vector spaces, and we have

$$\mathbf{k}_L=\left(\frac{2\pi\mu_{Lx}}{L_x},\frac{2\pi\mu_{Ly}}{L_y},\frac{2\pi\mu_{Lz}}{L_z}\right),\qquad \mathbf{k}=\left(\frac{2\pi\mu_x}{L_x},\frac{2\pi\mu_y}{L_y},\frac{2\pi\mu_z}{L_z}\right), \tag{5}$$

with $\mu_{Lx,y,z}$ and $\mu_{x,y,z}$ positive integers. Here L_x,L_y,L_z determine the size of the plasma, or the periodicity length; for example, they can be taken to be equal to the maximal wavelength of the electrostatic wave. The sums exclude the zero components, since they do not contribute to the equations of motion.

Although we have chosen a Fourier representation, the procedure is flexible enough to accommodate the use of a different set of basis functions depending on the geometry of the specific problem. For example, a plasma channel formed by an intense laser pulse has a cylindrical shape, so decomposition of the fields in a cylindrical geometry would be more appropriate. Also, one could build pulse shapes with many or few dynamic parameters that more realistically describe what is typically seen in experiments.

With the Fourier representation, the Coulomb gauge condition reads $\mathbf{k}\cdot\mathbf{a}_{\mathbf{k}}=0$. We assume the amplitudes $f_{\mathbf{k}_L}$ and $\mathbf{a}_{\mathbf{k}}$ contain slow and fast time scales, and consequently the derivatives will be given by

$$\dot{f}_{\mathbf{k}_L}=-i\omega_{\mathbf{k}_L}f_{\mathbf{k}_L}+\underline{\dot{f}}_{\mathbf{k}_L},\qquad \dot{\mathbf{a}}_{\mathbf{k}}=-i\omega_{\mathbf{k}}\mathbf{a}_{\mathbf{k}}+\underline{\dot{\mathbf{a}}}_{\mathbf{k}}. \tag{6}$$

Here the underline notation means differentiation with respect to the slow time scale, i.e., if $f_{\mathbf{k}_L}(t)=F_{\mathbf{k}_L}(t)e^{-i\omega_{\mathbf{k}_L}t}$, with $F_{\mathbf{k}_L}(t)$ representing the slow time dependence, then $\underline{\dot{f}}_{\mathbf{k}_L}(t)=\dot{F}_{\mathbf{k}_L}(t)e^{-i\omega_{\mathbf{k}_L}t}$. The second derivatives assume the form

$$\ddot{f}_{\mathbf{k}_L}=(-i\omega_{\mathbf{k}_L})^2f_{\mathbf{k}_L}-2i\omega_{\mathbf{k}_L}\underline{\dot{f}}_{\mathbf{k}_L}+\underline{\ddot{f}}_{\mathbf{k}_L}\simeq-\omega_{\mathbf{k}_L}^2f_{\mathbf{k}_L}-2i\omega_{\mathbf{k}_L}\underline{\dot{f}}_{\mathbf{k}_L},\qquad \ddot{\mathbf{a}}_{\mathbf{k}}\simeq-\omega_{\mathbf{k}}^2\mathbf{a}_{\mathbf{k}}-2i\omega_{\mathbf{k}}\underline{\dot{\mathbf{a}}}_{\mathbf{k}}, \tag{7}$$

where the second derivatives with respect to the slow time scale are neglected, according to the slow variation assumption; in particular, it is assumed that

$$|\underline{\ddot{f}}_{\mathbf{k}_L}|\ll\omega_{\mathbf{k}_L}|\underline{\dot{f}}_{\mathbf{k}_L}|\ll\omega_{\mathbf{k}_L}^2|f_{\mathbf{k}_L}|,\qquad |\underline{\ddot{\mathbf{a}}}_{\mathbf{k}}|\ll\omega_{\mathbf{k}}|\underline{\dot{\mathbf{a}}}_{\mathbf{k}}|\ll\omega_{\mathbf{k}}^2|\mathbf{a}_{\mathbf{k}}|.$$

Now Eqs. (2)–(7) are substituted into Eq. (1). The cold plasma dispersion relations, $\omega_{\mathbf{k}_L}^2=\omega_p^2$ for electrostatic and $\omega_{\mathbf{k}}^2=\omega_p^2+\mathbf{k}^2c^2$ for electromagnetic waves, and the formulas

for the derivatives, Eqs. (6) and (7), are used. The integration is performed over a domain with periodic boundary conditions. Upon integrating the squares, terms that contain different wave vectors in the exponential $e^{i(\mathbf{k}\pm\mathbf{k}')\cdot\mathbf{r}}$ average to zero, and so do terms in which the wave vectors double, $e^{\pm 2i\mathbf{k}\cdot\mathbf{r}}$. Only terms with equal wave vectors but opposite sign of the exponent survive, and for them the integration reduces to multiplication by the volume of integration. Use is made of the Coulomb gauge condition to reduce the vector products to scalar products. Details of the calculations are given in Appendix A, where the Lagrangian (1) is shown to take the following form:

$$
\begin{aligned}
L = & -mc^2 \sum_{j=1}^{N} \sqrt{1-\frac{\dot{\mathbf{r}}_j^2}{c^2}} + e\sum_{j=1}^{N}\sum_{\mathbf{k}_L>0}\left(f_{\mathbf{k}_L} e^{i\mathbf{k}_L\cdot\mathbf{r}_j} + f_{\mathbf{k}_L}^* e^{-i\mathbf{k}_L\cdot\mathbf{r}_j}\right) \\
& - \frac{e}{c}\sum_{j=1}^{N}\sum_{\mathbf{k}>0}\dot{\mathbf{r}}_j\cdot\left(\mathbf{a}_{\mathbf{k}} e^{i\mathbf{k}\cdot\mathbf{r}_j} + \mathbf{a}_{\mathbf{k}}^* e^{-i\mathbf{k}\cdot\mathbf{r}_j}\right) \\
& - \frac{V}{2\pi}\sum_{\mathbf{k}_L>0}\mathbf{k}_L^2\left(f_{\mathbf{k}_L} f_{\mathbf{k}_L}^*\right) + \frac{V}{4i\pi}\sum_{\mathbf{k}_L>0}\frac{\mathbf{k}_L^2}{\omega_p}\left(f_{\mathbf{k}_L}\dot{f}_{\mathbf{k}_L}^* - f_{\mathbf{k}_L}^*\dot{f}_{\mathbf{k}_L}\right) \\
& - \frac{V}{2\pi}\sum_{\mathbf{k}>0}\frac{\omega_{\mathbf{k}}^2}{c^2}\left(\mathbf{a}_{\mathbf{k}}\cdot\mathbf{a}_{\mathbf{k}}^*\right) + \frac{V}{4i\pi}\sum_{\mathbf{k}>0}\frac{\omega_{\mathbf{k}}}{c^2}\left(\mathbf{a}_{\mathbf{k}}\cdot\dot{\mathbf{a}}_{\mathbf{k}}^* - \mathbf{a}_{\mathbf{k}}^*\cdot\dot{\mathbf{a}}_{\mathbf{k}}\right).
\end{aligned}
\tag{8}
$$

The time scales implicit in Eq. (8) require further discussion. In the single-wave model, Refs. 1 and 2, the slow time scale in the system is obtained by a Galilean transformation to a frame moving with the initial beam velocity, or by a particular choice of variables. However, here this is not done because instead of a Galilean transformation, a Lorentz transformation should be used and that would involve transformation of the fields as well. It is preferable that the fields be the ones in the laboratory (stationary) frame. All quantities in this Lagrangian contain both the fast time scale, on the order of the electron plasma period, and the slow time scale, on which we assumed the amplitudes and phases of the waves vary. To obtain a quantity that varies on the slow time scale, we simply take instead of $f_{\mathbf{k}_L}$ and $\mathbf{a}_{\mathbf{k}}$, $|f_{\mathbf{k}_L}|$ and $|\mathbf{a}_{\mathbf{k}}|$.

A different way for averaging the Lagrangian over the fast time scale and retaining only the slow time scale has been followed by several authors.[12–14] It results in retaining only terms for which the resonant condition

$$
\mathbf{v}_0\cdot\mathbf{k}_L - \omega_p = 0 \tag{9}
$$

is satisfied. Indeed, the terms with $f_{\mathbf{k}_L}$ contain a time dependence of the form $e^{i(\mathbf{v}_0\cdot\mathbf{k}_L-\omega_p)t}$. If the phase velocity of the longitudinal wave equals that of the beam electrons, $\omega_p/k_L = v_0$, averaging over the time scale determined by ω_p and retaining the next-order small corrections (remember we have terms in the Lagrangian that contain small derivatives of amplitudes, and are therefore small compared to the rest of the terms) will result in only terms of zero- and first order in $(n/n_b)^{1/3}$, a quantity that is proportional to the ratio of the fast and slow time scales. Now consider the electromagnetic terms for which the fast time dependence has the form $e^{i(\mathbf{v}_0\cdot\mathbf{k}-\omega_{\mathbf{k}})t}$. In this case the resonant condition (9) cannot be satisfied, because the phase velocity of the electromagnetic wave is always greater than the speed of light (recall that $\omega_{\mathbf{k}}^2 = \omega_p^2 + \mathbf{k}^2c^2$). However, terms with electromagnetic waves can still produce slowly varying quantities. For example, if more than one electromagnetic wave is present then their frequencies can be chosen such that the resultant beat wave fulfills the necessary resonant condition. This case will be considered in Sec. III.

To continue, it is convenient to write all variables in dimensionless form. We use formula (5) to define the dimensionless coordinates and longitudinal wave vectors as $\mathbf{k}_L\cdot\mathbf{r}_j = \boldsymbol{\mu}_L\cdot\boldsymbol{\rho}_j$, and similarly for the transverse wave vectors, $\mathbf{k}\cdot\mathbf{r}_j = \boldsymbol{\mu}\cdot\boldsymbol{\rho}_j$. The time scale is given by $1/\omega_p$ and the length scale by the maximal longitudinal wavelength, i.e., we choose $L_x = L_y = L_z = 2\pi/|\mathbf{k}_{L_{\min}}|$. We define the dimensionless parameter $\beta = \omega_p/c|\mathbf{k}_{L_{\min}}|$, which is nearly the relativistic β, because the phase velocity of the plasma wave is nearly equal to the beam velocity and consequently is a measure of the importance of relativistic effects. The dimensionless electrostatic potential and vector potentials are given by

$$
f_{\mathbf{k}_L} = \frac{mc^2 s_{\boldsymbol{\mu}_L} f_{\boldsymbol{\mu}_L}}{e}, \quad \mathbf{a}_{\mathbf{k}} = \frac{mc^2 s_{\boldsymbol{\mu}}\mathbf{a}_{\boldsymbol{\mu}}}{e}. \tag{10}
$$

Greek letter subscripts are used to denote dimensionless variables and the dimensionless coefficients $s_{\boldsymbol{\mu}_L}$ and $s_{\boldsymbol{\mu}}$ are given by

$$
s_{\boldsymbol{\mu}_L} = \sqrt{\beta^2 n_b/2Nn\boldsymbol{\mu}_L^2}, \quad s_{\boldsymbol{\mu}} = \sqrt{n_b/2Nn\omega_{\boldsymbol{\mu}}}, \tag{11}
$$

where $\omega_{\boldsymbol{\mu}} = \omega_{\mathbf{k}}/\omega_p = (1+\boldsymbol{\mu}^2/\beta^2)^{1/2}$. Rescaling by mc^2 and V, the dimensionless Lagrangian is obtained:

$$
\begin{aligned}
L = & -\sum_{j=1}^{N}\sqrt{1-|\beta\dot{\boldsymbol{\rho}}_j|^2} + \sum_{j=1}^{N}\sum_{\boldsymbol{\mu}_L>0} s_{\boldsymbol{\mu}_L}\left(f_{\boldsymbol{\mu}_L} e^{i\boldsymbol{\mu}_L\cdot\boldsymbol{\rho}_j}\right. \\
& \left. + f_{\boldsymbol{\mu}_L}^* e^{-i\boldsymbol{\mu}_L\cdot\boldsymbol{\rho}_j}\right) - \sum_{j=1}^{N}\beta\dot{\boldsymbol{\rho}}_j\cdot\sum_{\boldsymbol{\mu}>0} s_{\boldsymbol{\mu}}\left(\mathbf{a}_{\boldsymbol{\mu}} e^{i\boldsymbol{\mu}\cdot\boldsymbol{\rho}_j} + \mathbf{a}_{\boldsymbol{\mu}}^* e^{-i\boldsymbol{\mu}\cdot\boldsymbol{\rho}_j}\right) \\
& - \sum_{\boldsymbol{\mu}_L>0}\left(f_{\boldsymbol{\mu}_L} f_{\boldsymbol{\mu}_L}^*\right) + \frac{1}{2i}\sum_{\boldsymbol{\mu}_L>0}\left(f_{\boldsymbol{\mu}_L}\dot{f}_{\boldsymbol{\mu}_L}^* - f_{\boldsymbol{\mu}_L}^*\dot{f}_{\boldsymbol{\mu}_L}\right) \\
& - \sum_{\boldsymbol{\mu}>0}\omega_{\boldsymbol{\mu}}\left(\mathbf{a}_{\boldsymbol{\mu}}\cdot\mathbf{a}_{\boldsymbol{\mu}}^*\right) + \frac{1}{2i}\sum_{\boldsymbol{\mu}>0}\left(\mathbf{a}_{\boldsymbol{\mu}}\cdot\dot{\mathbf{a}}_{\boldsymbol{\mu}}^* - \mathbf{a}_{\boldsymbol{\mu}}^*\cdot\dot{\mathbf{a}}_{\boldsymbol{\mu}}\right).
\end{aligned}
\tag{12}
$$

Observe that the field variables are either multiplied by small coefficients or contain a small slow time scale derivative. The small coefficients in front of the electrostatic variables depend on the ratio of beam and background plasma densities and on β, whereas those in front of the electromagnetic variables depend, in addition, on the inverse of the large number $\omega_{\boldsymbol{\mu}}$. It follows that the coupling of fields and particles is stronger for fast particles and for denser beams. The coupling between electromagnetic waves and particles is stronger for smaller frequency ratios $\omega_{\boldsymbol{\mu}}$.

As shown in Ref. 1, the single-wave model (without electromagnetic waves) is valid only when the condition $(n_b/n) \ll 1$ is satisfied; we require a relativistic version of this condition for our model:

$$(n_b/n) \ll 1/\gamma^{1/2}. \tag{13}$$

In addition, when electromagnetic waves are present in the system, the nonlinear response of the background plasma can be neglected if

$$a_0 \equiv \left| \frac{e\mathbf{A}}{mc^2} \right| \ll 1. \tag{14}$$

To see this, consider the linear response of the plasma, which yields a velocity that is linear in the electric field, $v_k^{(1)} \sim (ie/\omega_k m_e)E_k$; the nonlinear response is quadratic with respect to the fields, $v_k^{(2)} \sim (e^2/2m^2\omega_k^3)E_k^2$ (see Ref. 15). Upon using $\mathbf{E}_T=(1/c)\partial\mathbf{A}/\partial t=(\omega_k/c)\mathbf{A}$, the condition that the linear velocity be much larger than the nonlinear (quadratic) velocity, $v_k^{(1)} \gg v_k^{(2)}$, yields Eq. (14). The quantity on the left-hand side of Eq. (14) is the so-called normalized vector potential. In experiments on wakefield acceleration, a powerful laser pulse can have a normalized vector potential of the order unity or even larger. Our model would not be expected to be applicable to such experiments.

Condition (14) is necessary for neglecting the nonlinear response of the background plasma on the short plasma oscillation time scale. There are additional restrictions that apply when slower time scale effects are considered. For example, since we consider only long laser pulses, the ponderomotive force on the background plasma may be significant. In our model this force is neglected. If we consider pulses with spot radii much greater than the plasma wavelength then the transverse ponderomotive force will be negligible. If the laser pulse rises very slowly then the longitudinal ponderomotive force will be likewise small. Pulses that rise over several plasma wavelengths have been considered in the context of accelerators in the self-modulated regime.[16,17] The longitudinal ponderomotive force then causes a modulation of the laser pulse on the plasma oscillation time scale. This instability can be very fast growing if the pulse exceeds the critical power for relativistic optical guiding. For pulse powers below this critical power, the instability grows on the same time scale as that for forward Raman scattering.[17,18] If the pulse is very long (longer than 10–20 plasma wavelengths), the Raman instability can severely distort the pulse.[19] The processes considered in the present work grow faster than forward Raman scattering, provided the normalized vector potential is small enough. To see this, we compare the growth rate of the forward Raman scattering with that of the beam-plasma instability. The former has a growth rate $\gamma_{\text{forward}}=a_0\omega_p^2/2\sqrt{2}\omega$ (cf. Ref. 20), while the latter has a growth rate $\gamma_{\text{beam}}=(\sqrt{3}/2)\times(n_b/n)^{1/3}(\omega_p/\gamma)$ (cf. Ref. 2). The requirement that $\gamma_{\text{forward}} \ll \gamma_{\text{beam}}$ yields the condition

$$a_0 \ll \frac{\sqrt{6}}{\gamma}\frac{\omega}{\omega_p}\left(\frac{n_b}{n}\right)^{1/3}. \tag{15}$$

Another instability, backward Raman scattering, grows faster than forward Raman scattering. However, this instability saturates at very low levels (cf. Ref. 21), and thus we have excluded it from our model.

Summarizing, our model applies to broad and relatively long laser pulses with slow rise times and with power less than the critical power for relativistic optical self-guiding. Conditions (13)–(15), also need to be satisfied. We should note that not all simulations presented here satisfy the validity conditions just described. The reason we have chosen such particular initial conditions is that the phenomena under consideration are more clearly pronounced and thus better illustrate the presentation.

Given the Lagrangian formulation presented in this section, we can obtain the associated Hamiltonian formulation and conservation laws. We do this next in the following section.

B. Hamiltonian form and conservation laws

The Hamiltonian of the system is found from the Lagrangian (12) by Legendre transform. The canonical momentum is given by

$$\boldsymbol{\pi}_j = \partial L/\partial\dot{\boldsymbol{\rho}}_j = \frac{\beta^2\dot{\boldsymbol{\rho}}_j}{\sqrt{1-\beta^2\dot{\boldsymbol{\rho}}_j^2}} - \beta\sum_{\boldsymbol{\mu}>0} s_{\boldsymbol{\mu}}(\mathbf{a}_{\boldsymbol{\mu}}e^{i\boldsymbol{\mu}\cdot\boldsymbol{\rho}_j} + \mathbf{a}_{\boldsymbol{\mu}}^* e^{-i\boldsymbol{\mu}\cdot\boldsymbol{\rho}_j}). \tag{16}$$

For convenience, we introduce the notations

$$\begin{aligned} a_{j\sigma} &= \sum_{\boldsymbol{\mu}>0} s_{\boldsymbol{\mu}}(a_{\boldsymbol{\mu}\sigma}e^{i\boldsymbol{\mu}\cdot\boldsymbol{\rho}_j} + a_{\boldsymbol{\mu}\sigma}^* e^{-i\boldsymbol{\mu}\cdot\boldsymbol{\rho}_j}), \\ \mathbf{a}_{,j\sigma} &= \sum_{\boldsymbol{\mu}>0} is_{\boldsymbol{\mu}}(a_{\boldsymbol{\mu}\sigma}e^{i\boldsymbol{\mu}\cdot\boldsymbol{\rho}_j} - a_{\boldsymbol{\mu}\sigma}^* e^{-i\boldsymbol{\mu}\cdot\boldsymbol{\rho}_j})\boldsymbol{\mu}, \\ \mathbf{f}_{,j} &= \sum_{\boldsymbol{\mu}_L>0} is_{\boldsymbol{\mu}_L}(f_{\boldsymbol{\mu}_L}e^{i\boldsymbol{\mu}_L\cdot\boldsymbol{\rho}_j} - f_{\boldsymbol{\mu}_L}^* e^{-i\boldsymbol{\mu}_L\cdot\boldsymbol{\rho}_j})\boldsymbol{\mu}_L, \quad \sigma=1,2,3. \end{aligned} \tag{17}$$

Notice that the vectorial nature of $\mathbf{a}_{,j\sigma}$ and $\mathbf{f}_{,j}$ comes from $\boldsymbol{\mu}$ and $\boldsymbol{\mu}_L$, respectively. From Eq. (16)

$$\dot{\boldsymbol{\rho}}_j = \frac{1}{\beta}\frac{\boldsymbol{\pi}_j/\beta + \mathbf{a}_j}{\sqrt{1+(\boldsymbol{\pi}_j/\beta+\mathbf{a}_j)^2}}, \tag{18}$$

and using Eqs. (16) and (18) for the particle variables, the Hamiltonian is found to be

$$\begin{aligned} H = &\sum_{j=1}^{N}\sqrt{1+\left|\boldsymbol{\pi}_j/\beta + \sum_{\boldsymbol{\mu}>0} s_{\boldsymbol{\mu}}(\mathbf{a}_{\boldsymbol{\mu}}e^{i\boldsymbol{\mu}\cdot\boldsymbol{\rho}_j} + \mathbf{a}_{\boldsymbol{\mu}}^* e^{-i\boldsymbol{\mu}\cdot\boldsymbol{\rho}_j})\right|^2} \\ &- \sum_{j=1}^{N}\sum_{\boldsymbol{\mu}_L>0} s_{\boldsymbol{\mu}_L}(f_{\boldsymbol{\mu}_L}e^{i\boldsymbol{\mu}_L\cdot\boldsymbol{\rho}_j} + f_{\boldsymbol{\mu}_L}^* e^{-i\boldsymbol{\mu}_L\cdot\boldsymbol{\rho}_j}) \\ &+ \sum_{\boldsymbol{\mu}_L>0}(f_{\boldsymbol{\mu}_L}f_{\boldsymbol{\mu}_L}^*) + \sum_{\boldsymbol{\mu}>0}\omega_{\boldsymbol{\mu}}(\mathbf{a}_{\boldsymbol{\mu}}\cdot\mathbf{a}_{\boldsymbol{\mu}}^*), \end{aligned} \tag{19}$$

with Poisson brackets

$$\begin{aligned} &[\rho_{i\sigma}, \pi_{j\sigma'}] = \delta_{ij}\delta_{\sigma\sigma'}, \\ &[f_{\boldsymbol{\mu}_L}, f_{\boldsymbol{\mu}_L'}^*] = \frac{1}{i}\delta_{\boldsymbol{\mu}_L\boldsymbol{\mu}_L'}, \quad [a_{\boldsymbol{\mu}\sigma}, a_{\boldsymbol{\mu}'\sigma'}^*] = \frac{1}{i}\delta_{\boldsymbol{\mu}\boldsymbol{\mu}'}\delta_{\sigma\sigma'}, \end{aligned} \tag{20}$$

where $\sigma=1,2,3$. Notice that the brackets for the field variables differ from the canonical brackets only by a factor of $1/i$. The calculation for the Legendre transform of the field

part of the Hamiltonian is done in Appendix B.

The equations of motion that follow from Eq. (19) are

$$\dot{\boldsymbol{\rho}}_j = \frac{1}{\beta}\frac{\boldsymbol{\pi}_j/\beta + \mathbf{a}_j}{\sqrt{1+(\boldsymbol{\pi}_j/\beta+\mathbf{a}_j)^2}},$$

$$\dot{\boldsymbol{\pi}}_j = -\frac{(\boldsymbol{\pi}_{j\sigma}/\beta + a_{j\sigma})\mathbf{a}_{,j\sigma}}{\sqrt{1+(\boldsymbol{\pi}_j/\beta+\mathbf{a}_j)^2}} + \mathbf{f}_{,j},$$

$$\dot{f}_{\boldsymbol{\mu}_L} = -if_{\boldsymbol{\mu}_L} + \sum_{j=1}^{N} is_{\boldsymbol{\mu}_L} e^{-i\boldsymbol{\mu}_L\cdot\boldsymbol{\rho}_j}, \tag{21}$$

$$\dot{\mathbf{a}}_{\boldsymbol{\mu}} = -i\omega_{\boldsymbol{\mu}}\mathbf{a}_{\boldsymbol{\mu}} - \sum_{j=1}^{N} is_{\boldsymbol{\mu}} e^{-i\boldsymbol{\mu}\cdot\boldsymbol{\rho}_j}\frac{\boldsymbol{\pi}_j/\beta+\mathbf{a}_j}{\sqrt{1+(\boldsymbol{\pi}_j/\beta+\mathbf{a}_j)^2}},$$

and two equations that are complex conjugates of the last two. Summation over the repeated index σ in the second equation of Eqs. (21) is assumed. In addition to Eqs. (21), the gauge condition $\boldsymbol{\mu}\cdot\mathbf{a}_{\boldsymbol{\mu}}=0$ must be added.

Note, the momentum equation has two terms. The first is a ponderomotivelike force due to the electromagnetic field, and the second describes the electrostatic interaction with the beam particles. It also shows that the particles are coupled to both, the electrostatic and the electromagnetic fields. Each of the field equations has two terms on the right-hand side. The first term is just the wave oscillation (varying on the fast time scale), whereas the second term describes the coupling of the plasma to the beam particles through the waves. The latter involves the small coefficients $s_{\boldsymbol{\mu}_L}$ and $s_{\boldsymbol{\mu}}$ and is responsible for the slowly changing amplitudes assumed at the beginning of the derivation.

It is easy to see that the total momentum of the system of particles and waves is conserved:

$$P = \sum_{j=1}^{N}\boldsymbol{\pi}_j + \sum_{\boldsymbol{\mu}_L>0}\boldsymbol{\mu}_L|f_{\boldsymbol{\mu}_L}|^2 + \sum_{\boldsymbol{\mu}>0}\boldsymbol{\mu}|\mathbf{a}_{\boldsymbol{\mu}}|^2 = \text{const}. \tag{22}$$

It is also obvious that the total energy composed of both the fields and the particles is a conserved quantity; this follows automatically because the Hamiltonian (19) does not have explicit time dependence.

The system of Eqs. (21) is highly nonlinear, and integrability is unlikely even for a single particle with one longitudinal wave and one transverse wave. However, the system with one particle and one longitudinal wave is integrable (see Ref. 3), but this is not so for one particle and one transverse wave. In the nonrelativistic limit, the chaotic behavior was noted in Ref. 10. Linear analysis can be done in the absence of electromagnetic waves and in one spatial dimension (see, e.g., Ref. 3). Further investigation is based on numerical solution, and this is done in the following section.

III. FEW WAVE MODELS

In this section, we use numerical simulation to investigate the influence of electromagnetic waves on the beam-plasma system. We show that the presence of one external electromagnetic wave stabilizes the beam-plasma instability. When two external electromagnetic waves are present simultaneously, beat-wave resonance is observed. This is used to suggest that particles may be accelerated via the transfer of energy from the electromagnetic waves, since the relativistic particles and the beat wave can have matching velocities and thus can satisfy a resonance condition. Transfer of energy from the external electromagnetic waves to the plasma wave (through the beam particles) is observed only when a certain value of the initial vector potential, a certain threshold, is exceeded.

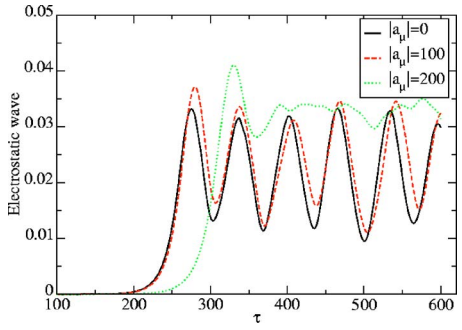

FIG. 1. (Color online). Simulation results with one electrostatic wave, one electromagnetic wave, and 100 particles with parameters $\mu=5$, $\beta=0.1$, and $n_b/n=10^{-3}$.

The numerical simulations are done with fourth-order Runge-Kutta method with an adaptive time step. The time step is controlled by the greater of the absolute error, which is the C^2 norm of the vector made up from all dependent variables and the relative error of the electrostatic field amplitude (this was chosen since the electrostatic field initial condition is a very small perturbation). The runs are done with accuracies usually of the order of 10^{-5}–10^{-6}. The difference in runs using two different accuracies is extremely small and only shows up at very long times. As expected, the system exhibits chaotic nature (see also Refs. 10 and 22).

A. One electrostatic wave and one electromagnetic wave

First, consider the beam-plasma system with one electromagnetic wave, and with dependence in one spatial dimension; i.e., all variables are assumed to depend on one spatial coordinate z and time. For our computer runs we take $N=100$ particles, $\boldsymbol{\mu}_L=(0,0,\mu_L)$, $\boldsymbol{\mu}=(0,0,\mu)$ with $\mu_L=1$, $\mu=2,3,\ldots$, and $n_b/n=0.001$. The dimensionless coefficients (11) have the order of magnitude values of $s_{\boldsymbol{\mu}}\simeq 2.2\times10^{-3}\sqrt{\beta/\mu}$ and $s_{\boldsymbol{\mu}_L}\simeq 2.2\times10^{-3}\beta/\mu_L$. For an estimate of how large the normalized vector potential $a_0=s_\mu a_\mu$ [see Eq. (10)] is for these values of the parameters, let us take $\mu=k_zL_z/2\pi=5$ and $\beta=\omega_p/c|\mathbf{k}_{L_{\min}}|=2\pi\omega_pL_z/c=0.1$. Then for $|\mathbf{a}_{\boldsymbol{\mu}}|=50$, $a_0=0.016$; for $|\mathbf{a}_{\boldsymbol{\mu}}|=400$, $a_0=0.12$. It is also clear that for larger β, a_0 has a larger value. For example, if $\beta=0.96$ and $\mu=3$, for $|\mathbf{a}_{\boldsymbol{\mu}}|=20$, $a_0=0.025$, and for $|\mathbf{a}_{\boldsymbol{\mu}}|=200$, $a_0=0.25$.

In Fig. 1, numerical solutions with one electrostatic wave and one electromagnetic wave are given for several different values of the transverse amplitude. It is seen that a larger amplitude of the electromagnetic wave causes a bit larger saturation amplitude for the electrostatic wave; how-

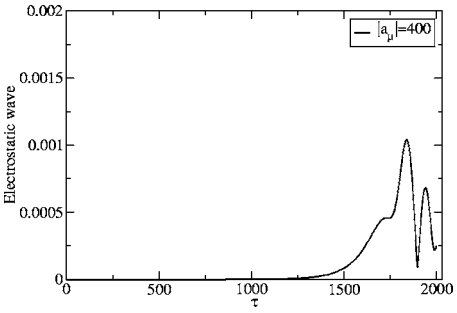

FIG. 2. Simulation results with one electrostatic wave and one electromagnetic wave with $\mu=5$, $\beta=0.1$, and $n_b/n=10^{-3}$. For larger amplitude of the electromagnetic wave a stabilizing influence on the electrostatic wave is seen.

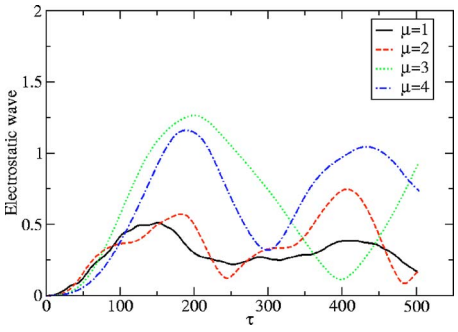

FIG. 3. (Color online). Electrostatic wave in the presence of two electromagnetic waves with $|\mathbf{a}_{\boldsymbol{\mu}}|=200$, $\beta=0.961$, and $n_b/n=10^{-3}$.

ever, at the same time there is a tendency to destroy the regularity of the oscillation. Notice also that for $|\mathbf{a}_{\boldsymbol{\mu}}|=200$, there is a significant delay of the onset of instability. In Fig. 2, the electromagnetic wave has even larger amplitude. As a result, a stabilizing effect is observed: the delay in the growth of the electrostatic wave is very significant, and the amplitude of saturation of the electrostatic wave is more than an order of magnitude smaller than that for $|\mathbf{a}_{\boldsymbol{\mu}}|=0$.

This behavior can be explained by analogy with the forced mathematical pendulum. The pendulum's unstable upright equilibrium point becomes stable when an external periodic force of a certain frequency is applied.[23] This suggests an important idea: to good approximation, the electromagnetic waves can be considered as an external force on the system of beam particles and electrostatic waves, and their amplitudes can be assumed to be constant. This idea will be used in a future work to draw some analytical conclusions about the system of Eqs. (21). In particular, this system will be further simplified to a one-and-a-half degrees of freedom system using the so-called macroparticle model of Ref. 3. This simplified system will be studied via the surfaces of section method and it will be shown that the portions of the curves in Figs. 6 and 7 below the threshold correspond to island deformation, whereas the threshold itself signifies island breaking. Transfer of energy is possible when phase space mixing occurs (Ref. 22).

B. Two electromagnetic and one electrostatic waves

A single electromagnetic wave has a phase velocity greater than the speed of light, and therefore cannot be used to resonantly drive the beam particles. On the other hand, if two waves are present, their frequencies and wave vectors can be chosen to satisfy

$$\omega_{\mathbf{k}+\mathbf{k}_L}-\omega_{\mathbf{k}}=\omega_p. \tag{23}$$

Such a matching condition can be used to obtain resonant driving of the plasma wave (and the beam particles). To see if this holds for the system of Eqs. (21), we expand the above matching condition for $\mu_L/\mu \ll 1$ and use the definition of $\beta=\omega_p/k_L c$ to obtain

$$\mu^2+\mu-\frac{\beta^2}{2(1-\beta)}=0. \tag{24}$$

This quadratic equation, if solved for β with given values of μ, gives values for the matching condition. For example, if $\mu=1$, the solution yields a value $\beta=0.83$. The electromagnetic waves must have higher frequency than the electrostatic wave in order to propagate in the plasma. Therefore, if $\mu \geqslant 1$, the above value of β is a lower bound on the beam velocity for which the matching condition (23) can be satisfied. Table I gives values of β as a function of μ defined by Eq. (24). To test for beat-wave resonance, we choose different values of μ and fix β to equal some of the values in Table I. We expect to observe a resonant curve similar to that of a forced pendulum.[23]

The plots in Fig. 3 show how the amplitude of the plasma wave is affected by the presence of two electromagnetic waves with equal amplitudes, but different wave vectors. Only waves with $\mu=3$ and $\mu=4$ satisfy the matching condition, and we see that the electrostatic wave then has the largest saturation amplitude. The rest of the curves are slightly off resonance, but still have a much stronger influence than a single electromagnetic wave, as shown in Fig. 1.

TABLE I. Solutions of Eq. (24), relating β to various values of given μ.

μ	1	2	3	4	5
β	0.828	0.928	0.961	0.976	0.984

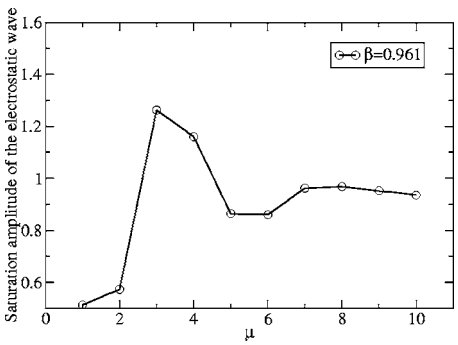

FIG. 4. Resonance curve for $\beta=0.961$, $|\mathbf{a}_{\boldsymbol{\mu}}|=200$, and $n_b/n=10^{-3}$.

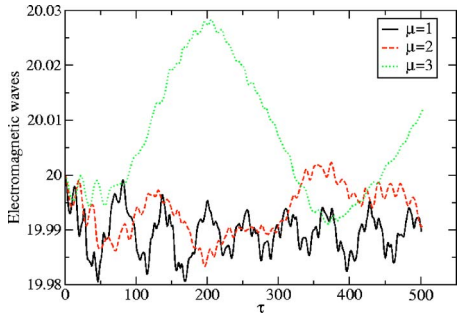

FIG. 5. (Color online). The change in the electromagnetic waves. The largest change is for the waves with $\mu_{1,2}=3,4$ that satisfy the matching condition (24) for $\beta=0.961$, $|\mathbf{a}_{\mu}|=200$, and $n_b/n=10^{-3}$.

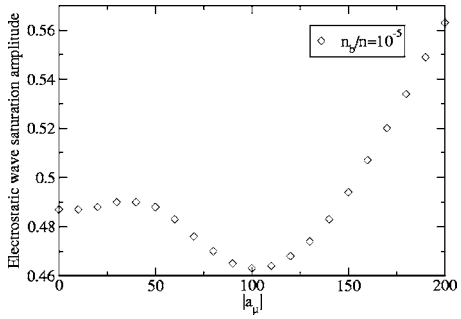

FIG. 7. Threshold of instability of the electrostatic wave in the presence of two electromagnetic waves with $\mu_{1,2}=3,4$; $\beta=0.961$; and $n_b/n=10^{-5}$.

In Fig. 4, we show the resonant curve, i.e., the saturation amplitude as a function of the electromagnetic waves' wave vector ($\omega_k/\omega_p \simeq \mu$). A clearly pronounced resonance is seen. In Fig. 5, we see that the electromagnetic waves with $\mu=3,4$ have the largest oscillation of their amplitudes. Note that we have plotted the electromagnetic wave amplitudes $|\mathbf{a}_{\mu}|/\sqrt{N}$ to make the plotted quantity independent of the number of beam particles. Since $N=100$, the scale on the graph shows 1/10th of the actual value of $|\mathbf{a}_{\mu}|$.

Next we study the change in the electrostatic wave saturation amplitude for small amplitudes of the electromagnetic waves. Figures 6 and 7 show this dependence. The two electromagnetic waves satisfy the matching condition (23). When the electromagnetic wave amplitudes are small, the electrostatic wave responds with a large phase shift, but with no significant change in its saturation amplitude (see Fig. 8). Only above the values of $|\mathbf{a}_{\mu}| \simeq 20$ for $n_b/n=10^{-3}$ and $|\mathbf{a}_{\mu}| \simeq 100$ for $n_b/n=10^{-5}$ does the electrostatic wave saturation amplitude increase steadily. Such a threshold is equivalent to an effective "loss" or "damping." In our Hamiltonian model there is no loss of energy in the system. However, recall that the electromagnetic and the electrostatic waves only interact with the beam particles and not with each other. The electromagnetic waves transfer momentum to the beam particles, thus heating the beam. However, a certain minimal value of the heating is required before the beam particles can transfer any energy to the electrostatic wave. This minimal value is determined by comparing the rates of heating by the electromagnetic waves and rate of transferring beam energy to the electrostatic wave. When the heating rate exceeds the rate of transfer of beam energy, the electrostatic wave gains energy from both the beam and the electromagnetic waves. The situation where a threshold exists in a system without energy loss is similar to that of plasma parametric instabilities in inhomogeneous medium: there is no loss of energy in the system, but a threshold for instability can arise from spatial inhomogeneities. If the region of instability is of the order of a plasma wavelength, and the electromagnetic wave period is close to the plasma wave period, energy can escape from the unstable region into the stable region on a time scale of a plasma period, and thus can provide an effective "loss" mechanism. This loss results in the existence of a threshold for the electromagnetic wave amplitude, below which a plasma wave cannot be excited (see Ref. 24).

It is important to emphasize that under the conditions described at the end of Sec. II A, the nonlinear interactions between the waves and the background plasma are weak. Therefore, the only means of coupling of electromagnetic waves with each other and with electrostatic waves is by means of the beam particles. The waves and particles must satisfy the matching condition (23). In our model the resonant particles are the beam particles. The simulations in Fig. 8 for beam-plasma density ratio 10^{-3} show amplification of about 6%. The amplification is expected to be higher for denser electron beams, because condition (15) would allow larger amplitudes a_0 whereas from Fig. 9 we see that the threshold for amplification stays almost constant and does

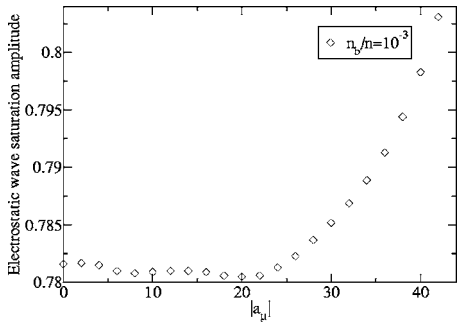

FIG. 6. Threshold of instability of the electrostatic wave in the presence of two electromagnetic waves with $\mu_{1,2}=3,4$; $\beta=0.961$; and $n_b/n=10^{-3}$.

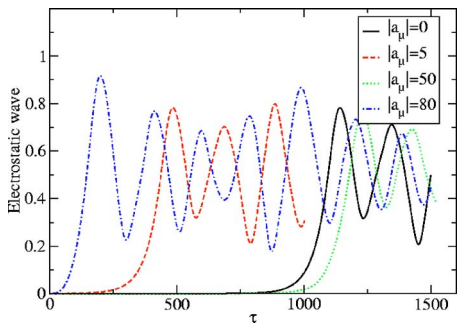

FIG. 8. (Color online). Resonant amplification and phase shift of an electrostatic wave in the presence of two electromagnetic waves with $|\mathbf{a}_{\mu}|=5,80$, and $\mu_1=3$, $\mu_2=4$. The curve with $|\mathbf{a}_{\mu}|=50$, $\mu_1=3$, $\mu_2=5$ does not satisfy the resonance condition (24) for $\beta=0.961$, and is seen not to cause any transfer of energy (amplification) to the electrostatic wave. In this figure $n_b/n=10^{-3}$.

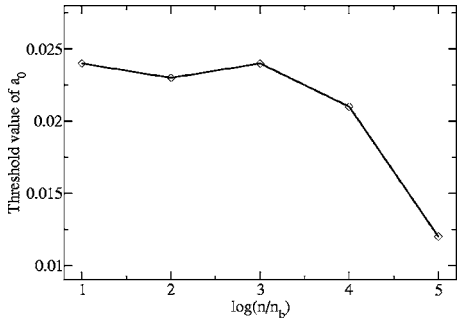

FIG. 9. Threshold for amplification of the plasma wave vs the logarithm (base 10) of the plasma-electron beam density ratio.

not exceed the value of $a_0=0.024$. In Fig. 8, $|a_\mu|=80$ corresponds to $a_0=0.1$ and formula (15) requires that it be less than 0.2. We see that the presence of a small beat wave has a significant effect on the instability process.

IV. CONCLUSIONS

We have presented a general method for reducing a complicated relativistic system of nonlinear field equations that describe beam electrons, plasma waves, and transverse electromagnetic waves to a finite-dimensional Hamiltonian system. The Hamiltonian structure makes clear the conservations laws and the interaction terms of the N beam particles, the N_L plasma waves, and the N_T transverse waves. The nonlinearity of the wave-particle interactions and the nonlinear beam particle orbits are kept, but the nonlinearity of the thermal background plasma is dropped.

We emphasize that the derivation procedure is flexible and can be adapted to accommodate general geometries and various pulse shapes, in better agreement with experimental conditions. Also, inclusion of additional physical effects, such as the ponderomotive force on the background plasma or the direct nonlinear coupling of the electrostatic and electromagnetic waves, can be done in a systematic way. The derived model describes physics of high-energy accelerators, features of laboratory and space plasmas, and laser-plasma interaction. Specific adaptation of the derivation procedure can be used to describe many phenomena, such as the acceleration of electrons by whistler waves in magnetospheric plasmas, a future calculation that we envision.

ACKNOWLEDGMENT

This work was supported by the U.S. Department of Energy under Contract No. DE-FG03-96ER-54346.

APPENDIX A: DETAILS OF THE DERIVATION

In this appendix we present the part of the derivation that only contains the vector potentials. First, consider the term in the Lagrangian (1) containing $|\mathbf{v}|^2$. Using formulas (2), (4), (6), and (7), and taking into account that $\mathbf{j}_L$ is perpendicular to $\mathbf{j}_T$ (only $\mathbf{j}_T$ contains the vector potential $\mathbf{A}$), we have

$$\begin{aligned}\int d^3x\frac{1}{2}mn|\mathbf{v}|^2 &= \frac{c^2}{8\pi\omega_p^2}\int d^3x\left|\nabla^2\mathbf{A}-\frac{1}{c^2}\frac{\partial^2\mathbf{A}}{\partial t^2}\right|^2\\ &= \frac{c^2}{8\pi\omega_p^2}\int d^3x\left|\sum_{\mathbf{k}>0}\left(\frac{\omega_\mathbf{k}^2}{c^2}-k^2\right)(\mathbf{a}_\mathbf{k}e^{i\mathbf{k}\cdot\mathbf{r}}\right.\\ &\quad +\mathbf{a}_\mathbf{k}^*e^{-i\mathbf{k}\cdot\mathbf{r}})+\frac{1}{c^2}[2i\omega_\mathbf{k}(\dot{\mathbf{a}}_\mathbf{k}e^{i\mathbf{k}\cdot\mathbf{r}}-\dot{\mathbf{a}}_\mathbf{k}^*e^{-i\mathbf{k}\cdot\mathbf{r}})\\ &\quad \left.-(\ddot{\mathbf{a}}_\mathbf{k}e^{i\mathbf{k}\cdot\mathbf{r}}+\ddot{\mathbf{a}}_\mathbf{k}^*e^{-i\mathbf{k}\cdot\mathbf{r}})]\right|^2\\ &\simeq \frac{Vc^2}{8\pi\omega_p^2}\sum_{\mathbf{k}>0}\left[2\left(\frac{\omega_p^2}{c^2}\right)^2|\mathbf{a}_\mathbf{k}|^2\right.\\ &\quad \left.-4i\frac{\omega_p^2}{c^2}\frac{\omega_\mathbf{k}}{c^2}(\mathbf{a}_\mathbf{k}\cdot\dot{\mathbf{a}}_\mathbf{k}^*-\dot{\mathbf{a}}_\mathbf{k}\cdot\mathbf{a}_\mathbf{k}^*)\right],\end{aligned}\tag{A1}$$

where $V=L_xL_yL_z=L_x^3$ is the volume of the system. Here we have neglected second-order time derivatives of $\mathbf{a}_\mathbf{k}$, as well as products of first-order time derivatives; the dispersion relation for electromagnetic waves has also been used. For the integration of the rest of the terms containing $\mathbf{A}$, note that the current term in the Lagrangian may be transformed so that it equals twice the field term with a negative sign. Therefore, for the rest of the calculation we need to evaluate as follows:

$$\begin{aligned}-\frac{1}{8\pi c^2}\int d^3x\left|\frac{\partial\mathbf{A}}{\partial t}\right|^2 &= \int d^3x\left|\sum_{\mathbf{k}>0}(-i\omega_\mathbf{k}(\mathbf{a}_\mathbf{k}e^{i\mathbf{k}\cdot\mathbf{r}}\right.\\ &\quad \left.-\mathbf{a}_\mathbf{k}^*e^{-i\mathbf{k}\cdot\mathbf{r}})+\dot{\mathbf{a}}_\mathbf{k}e^{i\mathbf{k}\cdot\mathbf{r}}+\dot{\mathbf{a}}_\mathbf{k}^*e^{-i\mathbf{k}\cdot\mathbf{r}})\right|^2\\ &\simeq -\frac{V}{8\pi c^2}\sum_{\mathbf{k}>0}[2\omega_\mathbf{k}^2|\mathbf{a}_\mathbf{k}|^2\\ &\quad -2i\omega_\mathbf{k}(\mathbf{a}_\mathbf{k}\cdot\dot{\mathbf{a}}_\mathbf{k}^*-\mathbf{a}_\mathbf{k}^*\cdot\dot{\mathbf{a}}_\mathbf{k})]\end{aligned}\tag{A2}$$

and

$$\begin{aligned}\frac{1}{8\pi}\int d^3x|\nabla\times\mathbf{A}|^2 &= \frac{1}{8\pi}\int d^3x\sum_{\mathbf{k}>0}|(i\mathbf{k}\times\mathbf{a}_\mathbf{k})e^{i\mathbf{k}\cdot\mathbf{r}}\\ &\quad -(i\mathbf{k}\times\mathbf{a}_\mathbf{k}^*)e^{-i\mathbf{k}\cdot\mathbf{r}}|^2\\ &= \frac{V}{8\pi}\sum_{\mathbf{k}>0}2k^2|\mathbf{a}_\mathbf{k}|^2.\end{aligned}\tag{A3}$$

In the last step the Coulomb gauge condition, $\mathbf{k}\cdot\mathbf{a}_\mathbf{k}=0$, was used. Adding Eqs. (A1)–(A3), we see that upon using the dispersion relation for electromagnetic waves, all terms with $|\mathbf{a}_\mathbf{k}|^2$ cancel and the remaining terms combine into

$$\frac{V}{4i\pi}\sum_{\mathbf{k}>0}\frac{\omega_\mathbf{k}}{c^2}(\mathbf{a}_\mathbf{k}\cdot\dot{\mathbf{a}}_\mathbf{k}^*-\dot{\mathbf{a}}_\mathbf{k}\cdot\mathbf{a}_\mathbf{k}^*).\tag{A4}$$

By an analogous calculation for the terms involving the electrostatic potential, one can show that upon using the cold plasma dispersion relation for electrostatic waves, terms with $|f_{\mathbf{k}_L}|^2$ cancel out and the remaining terms, after performing the integration over the spatial variables, are

$$\frac{V}{4i\pi}\sum_{\mathbf{k}_L>0}\frac{\mathbf{k}_L^2}{\omega_p}(f_{\mathbf{k}_L}\dot{\underline{f}}^*_{\mathbf{k}_L}-\dot{\underline{f}}_{\mathbf{k}_L}f^*_{\mathbf{k}_L}). \tag{A5}$$

To include Eqs. (A4) and (A5) into the Lagrangian (1), we make use of formulas (6) to express $\dot{\underline{\mathbf{a}}}_{\mathbf{k}}$ and $\dot{\underline{f}}_{\mathbf{k}_L}$ in terms of $\mathbf{a}_{\mathbf{k}}$, $\dot{\mathbf{a}}_{\mathbf{k}}$, $f_{\mathbf{k}_L}$, and $\dot{f}_{\mathbf{k}_L}$.

APPENDIX B: ACTION PRINCIPLE FOR THE WAVES

Consider an action principle of the form

$$S=\int dt[A_i(q)\dot{q}_i-V(q)], \tag{B1}$$

where we have used the repeated index summation convention and q denotes an even number of generalized coordinates. We would like to find the Hamiltonian equations and the Poisson bracket for this action. Let us vary the action (B1) with respect to all coordinates

$$\begin{aligned}\delta S&=\int dt\left(\frac{\partial A_i}{\partial q_j}\delta q_j\dot{q}_i+A_i(q)\delta\dot{q}_i-\frac{\partial V}{\partial q_i}\delta q_i\right)\\&=\int dt\left(\frac{\partial A_i}{\partial q_j}\delta q_j\dot{q}_i-\frac{d}{dt}[A_i(q)]\delta q_i-\frac{\partial V}{\partial q_i}\delta q_i\right)\\&=\int dt\left\{\left(\frac{\partial A_j}{\partial q_i}-\frac{\partial A_i}{\partial q_j}\right)\dot{q}_j-\frac{\partial V}{\partial q_i}\right\}\delta q_i=0.\end{aligned} \tag{B2}$$

If we require that the variation of S vanishes for every choice of δq_i then we obtain the equations of motion

$$-\Omega_{ij}\dot{q}_j=\frac{\partial V}{\partial q_i}, \tag{B3}$$

where we have defined

$$\Omega_{ij}=\left(\frac{\partial A_i}{\partial q_j}-\frac{\partial A_j}{\partial q_i}\right). \tag{B4}$$

If now suppose that the matrix Ω is invertible, we can define the matrix J by

$$J_{ij}=(-\Omega_{ij})^{-1}. \tag{B5}$$

We see that the matrix J is antisymmetric and has an even rank. Therefore, it can play the role of a Poisson bracket, whereas the Hamilton equations may be written as

$$\dot{q}_i=J_{ij}\frac{\partial V}{\partial q_i}. \tag{B6}$$

We can see that such system may be considered as Hamiltonian, where half of the coordinates play the role of generalized coordinates whereas the other half are the generalized momenta. Thus V is the Hamiltonian of the system and J is the Poisson bracket.

We apply this approach to the field part of the Lagrangian (12) to find the field part of the Hamiltonian, as well as the Poisson brackets that yield the equations of motion for the fields. The variables $f_{\mathbf{k}_L}$ and $\mathbf{a}_{\mathbf{k}}$ play the role of generalized coordinates, and their complex conjugate, $f^*_{\mathbf{k}_L}$ and $\mathbf{a}^*_{\mathbf{k}}$, are their conjugate momenta. Therefore, if we take the part of the Lagrangian which contains the fields (for example, let us consider only the vector potentials)

$$\begin{aligned}L_{\mathbf{a}}&=\frac{1}{2i}\sum_{\mu>0}(\mathbf{a}_{\boldsymbol{\mu}}\cdot\dot{\mathbf{a}}^*_{\boldsymbol{\mu}}-\mathbf{a}^*_{\boldsymbol{\mu}}\cdot\dot{\mathbf{a}}_{\boldsymbol{\mu}})-V(\mathbf{a})\\&=\frac{1}{2i}\sum_{\mu>0}\sum_{\sigma=1}^{3}(-a^*_{\boldsymbol{\mu}\sigma}\dot{a}_{\boldsymbol{\mu}\sigma}+a_{\boldsymbol{\mu}\sigma}\dot{a}^*_{\boldsymbol{\mu}\sigma})-V(\mathbf{a}).\end{aligned} \tag{B7}$$

Take $q_1=a_{\boldsymbol{\mu}1}$, $q_2=a^*_{\boldsymbol{\mu}1}$, $A_1=-a^*_{\boldsymbol{\mu}1}$, $A_2=a_{\mu1}$, etc. It is easy to see that the matrix Ω is block diagonal with a block for each pair of field variables $a_{\boldsymbol{\mu}\sigma},a^*_{\boldsymbol{\mu}\sigma}$. According to formula (B4) each block has the form

$$\Omega_{\boldsymbol{\mu}\sigma}=\frac{1}{2i}\begin{pmatrix}0&-2\\2&0\end{pmatrix}. \tag{B8}$$

Since the matrix $-\Omega_{\boldsymbol{\mu}\sigma}$ is just the σ_2 Pauli matrix, its inverse is itself and the Poisson bracket is determined by the cosymplectic form

$$J_{\boldsymbol{\mu}\sigma}=\begin{pmatrix}0&-i\\i&0\end{pmatrix}. \tag{B9}$$

[1] T. M. O'Neil, J. H. Winfrey, and J. H. Malmberg, Phys. Fluids **14**, 1204 (1971).
[2] N. G. Matsiborko, I. N. Onishchenko, V. D. Shapiro, and V. I. Shevchenko, Plasma Phys. **14**, 591 (1972).
[3] J. L. Tennyson, J. D. Meiss, and P. J. Morrison, Physica D **71**, 1 (1994).
[4] F. E. Low, Proc. R. Soc. London, Ser. A **248**, 282 (1959).
[5] R. L. Dewar, Phys. Fluids **13**, 2710 (1970).
[6] J. P. Dougherty, J. Plasma Phys. **4**, 761 (1970).
[7] H. Ye and P. J. Morrison, Phys. Fluids B **4**, 771 (1992).
[8] K. Sonnad and J. Cary, Phys. Rev. E **69**, 056501 (2004).
[9] P. J. Morrison, Phys. Plasmas **12**, 058102 (2005).
[10] E. G. Evstatiev, W. Horton, and P. J. Morrison, Phys. Plasmas **10**, 4090 (2003).
[11] J. D. Jackson, *Classical Electrodynamics*, 3rd ed. (Wiley, New York, 1999), p. 242.
[12] D. Bauer, P. Mulser, and W.-H. Steeb, Phys. Rev. Lett. **75**, 4622 (1995).
[13] M. D. Tokman, Plasma Phys. Rep. **25**, 140 (1999).
[14] I. Y. Dodin and N. J. Fisch, Phys. Rev. E **68**, 056402 (2003).
[15] V. N. Tsytovich, *Nonlinear Effects in Plasma*, 1st ed. (Plenum, New York, 1970), p. 26.
[16] J. Krall, A. Ting, E. Esarey, and P. Sprangle, Phys. Rev. E **48**, 2157 (1993).
[17] E. Esarey, J. Krall, and P. Sprangle, Phys. Rev. Lett. **72**, 2887 (1994).
[18] E. Esarey, J. Krall, P. Sprangle, and A. Ting, IEEE Trans. Plasma Sci. **24**, 252 (1996).
[19] T. M. Antonsen, Jr. and P. Mora, Phys. Rev. Lett. **69**, 2204 (1992).
[20] W. L. Kruer, *The Physics of Laser Plasma Interactions* (Addison-Wesley, Reading, MA, 1988), p. 79.
[21] P. Sprangle and E. Esarey, Phys. Rev. Lett. **67**, 2021 (1991).
[22] E. G. Evstatiev, Ph.D. thesis, The University of Texas at Austin, Austin, 2004.
[23] V. I. Arnold, *Ordinary Differential Equations*, 10th ed. (MIT Press, Cambridge, 1998), p. 207.
[24] F. W. Perkins and J. Flick, Phys. Fluids **14**, 2012 (1971).